# Radiofrequency thalamotomy for tremor produces focused and predictable lesions shown on magnetic resonance images

## Imaging radiofrequency thalamotomy lesions

Bryony K. Ishihara[1], Michael G. Hart[1], Thomas R. Barrick[1], Franklyn A. Howe[1], Francesca Morgante[1,2], Erlick A. Pereira[1]

[1] Neurosciences Research Centre, Molecular and Clinical Sciences Research Institute, St George's, University of London, London, United Kingdom.

[2] Department of Experimental and Clinical Medicine, University of Messina, Messina, Italy.

Correspondence to: Bryony K. Ishihara

Neurosciences Research Centre

St George's, University of London

Cranmer Terrance

London SW17 0RE

United Kingdom

Email: bishihar@sgul.ac.uk

**Abstract**

Radiofrequency (RF) thalamotomy is a neurosurgical management option for medically-refractory tremor. In this observational study, we evaluate the magnetic resonance imaging (MRI) features of the resultant lesion, their temporal dynamics, and how they vary depending on surgical factors. We report on lesion characteristics including size and location, as well as how these vary over time and across different MRI sequences.

Data from 12 patients (2 essential tremor, 10 Parkinson's disease) who underwent unilateral RF thalamotomy for tremor were analysed. Lesion characteristics were compared across 5 structural sequences. Volumetric analysis of lesion features was performed at early (< 5 weeks) and late (> 5 months) timepoints by manual segmentation. Lesion location was determined after registration of lesions to standard space.

All patients showed tremor improvement (clinical global impressions scale) post-operatively. Chronic side effects included balance disturbances (n=4) and worsening mobility due to parkinsonism progression (n=1). Early lesion features including a necrotic core, cytotoxic oedema and perilesional oedema were best demarcated on T2-weighted sequences. Multiple lesions were associated with greater cytotoxic oedema compared with single lesions (T2-weighted mean volume: 537 ± 112 $mm^3$ versus 302 ± 146 $mm^3$, p=0.028). Total lesion volume reduced on average by 90% between the early and late scans (T2-weighted mean volume: 918 ± 517 versus 75 ± 50 $mm^3$, t=3.592, p=0.023, n=5), with comparable volumes demonstrated at approximately 6 months after surgery. Lesion volumes on susceptibility-weighted images (SWI) were larger than those of T2-weighted images at later timepoints.

Radiofrequency thalamotomy produces focused and predictable lesion imaging characteristics over time. T2-weighted scans distinguish between the early lesion core and oedema characteristics, while lesions may remain more visible on SWI in the months following surgery. Scanning patients in the immediate post-operative period and then at 6 months is clinically meaningful for understanding the anatomical basis of the transient and permanent effects of thalamotomy.

Keywords: Thalamotomy, Parkinson's Disease, Essential tremor, lesion, magnetic resonance imaging

## Introduction

Tremor due to Parkinson's Disease (PD) and essential tremor (ET) is often inadequately managed with oral medication but responds well to neurosurgery.[1] Unilateral radiofrequency (RF) thalamotomy is an effective treatment for medically-refractory tremor involving lesioning of the ventral intermediate (VIM) nucleus of the thalamus.[2,3] While neurosurgical techniques such as deep brain stimulation (DBS) and magnetic resonance-guided focused ultrasound thalamotomy (MRgFUS) have become increasingly common in the treatment of movement disorders, RF thalamotomy remains an important therapeutic option owing to its simplicity, effectiveness, wealth of supporting clinical experience, and favourable health economics profile .[4–6]

Despite this experience, there are few studies on the magnetic resonance imaging (MRI) features of thalamic lesions created by RF, and to our knowledge there has been no comparison of different imaging sequences in defining RF thalamotomy lesions in humans. This study evaluated RF thalamotomy lesions using multiple MRI sequences to understand lesion characteristics and temporal dynamics, and how they varied depending on surgical factors. Our primary aims were to inform postoperative MR imaging protocols for future prospective studies, and to better understand lesion characteristics for comparison between different lesioning modalities e.g., MRgFUS.

## Materials and Methods

This study was approved by the National Research Ethics Service Local Research Ethics Committee (IRAS: 259146).

## Participants

A prospective series of patients between 2017-2022 discussed in the movement disorders multidisciplinary team (MDT) at St George's Hospital, London and deemed eligible for RF thalamotomy were identified retrospectively (n=14). Patient selection was based upon recognised criteria for DBS in movement disorders. Additionally, a radiofrequency lesion was favoured when the symptom impact was predominantly unilateral and there were extenuating medical co-morbidities that made general anaesthesia or implantation of a device less appealing. Finally, patient choice was a key criterion particularly if an immediate effect or reduction in visits for programming were meaningful. Two of these patients did not receive RF thalamotomy after testing and were therefore excluded.

## Surgical procedure

Stereotactic surgery was performed using a Cosman-Roberts-Wells (CRW) stereotactic frame (Integra, USA) under local anaesthesia while patients were fully awake. Targeting was performed using Renishaw Neuronspire™ (Renishaw plc, UK). Indirect co-ordinates 11-15 mm lateral and 4 mm posterior to the mid-commissural point (MCP) [7] were refined to ensure the target was approximately 10 mm from the lateral border of the 3rd ventricle on T2-weighted imaging and 2-3 mm from the medial internal capsule on fast grey matter acquisition T1 inversion recovery (FGATIR) at the level of the MCP (Z depth = 0).[8] A 2 mm diameter reusable radiofrequency thermocoagulation electrode with a 2 mm uninsulated tip (TC-16-2-250-D electrode and Cosman G4 generator; Boston Scientific Corporation, Marlborough, Massachusetts, USA) was inserted after twistdrill craniotomy.

Neurological assessment was performed in the awake patient by a board-certified consultant neurologist. Macrostimulation utilised the G4™ RF Generator (Boston Scientific Corporation, Valencia, CA, USA). Parameters included inhibitory testing at a frequency of 50Hz and pulse width of 0.5ms to identify voltage thresholds for capsular and sensory effects. Motor stimulation was performed at 2Hz and 0.5ms. Depth was adjusted with a CRW manual microdrive (Integra, USA) to identify tremor improvement based on clinical assessment and side-effect thresholds. Lesions were made by heating the electrode to 80°C. Lesioning parameters, specifically number of lesions and their duration, was determined based on the underlying symptoms, clinical response, and physiological effects viz a viz motor and sensory impairment. For example, with an early response to less severe symptoms our minimum duration was 30 seconds, while in another case with more severe tremor 3 lesions were used for a total of 210 seconds as they were well tolerated without side effects. If multiple lesions were considered our preference was to extend along the existing tract in the first instance, which was typically planned to allow safe progression into the zona incerta.

MRI acquisition

MR images were acquired on a 3.0 Tesla (3T) scanner with a 32-channel head coil (Philips dual Tx Acheiva, St George's Hospital). The clinical imaging procedure was to scan patients pre-operatively, and at 2 weeks and 6 months post-operatively. The MR imaging protocol included the following sequences: Magnetisation prepared rapid gradient echo (MPRAGE, T1-weighted, TR = 6.8 ms, TE = 3.1 ms, TI = 819 ms, flip angle = 8°, 1mm isotropic spatial resolution); T2-weighted (TR = 2200 ms, TE = 258 ms, flip angle = 90°, spatial resolution = 0.65 × 0.65 × 0.8 mm); fluid attenuated inversion recovery (FLAIR, TR = 6000 ms, TE = 274 ms, IR = 2200 ms = , flip angle = 40°, spatial resolution = 0.98 × 0.98 × 1 mm);

susceptibility-weighted imaging (SWI, TR = 22 ms, TE = 32 ms, flip angle = 15°, spatial resolution = 0.49 × 0.49 × 1 mm) and fast grey matter acquisition T1 inversion recovery (FGATIR, TR = 7.5 ms, TE = 3.5 ms, flip angle = 8°, spatial resolution = 0.625 × 0.625 × 1 mm).

## Clinical outcome

Patients were evaluated by a neurologist using the clinical global impressions (CGI) scale (measure of clinical improvement on a scale of 1 - very much improved, to 7 - very much worse) in post-operative day 0 and then at 3 and 12 months postoperatively. In depth structured assessments at multiple time points were not routinely performed in accordance with our aim of minimising logistical burdens in an often physically impaired patient cohort.

## Lesion analysis

Imaging analysis was performed using FSL (FMRIB Software Library v6.0).[9,10]

### *Expanding spherical signal intensity analysis*

Lesion appearances on different MR sequences were compared on a single patient by analysing their voxel-wise MRI signal intensities in native space. For each sequence (MPRAGE, T2-weighted, FLAIR, SWI and FGATIR), a seed coordinate was determined at the centre of the lesion. From this point, 11 spherical regions of interest (ROIs) were created with increasing radiuses (1-6 mm in increments of 0.5 mm). For each ROI, the previous ROI (radius smaller by 0.5 mm) was subtracted, and the mean signal intensity extracted (Fig 1). Signal intensity was then normalised by dividing by the mean intensity of the surrounding

intact tissue of the thalamus. This analysis was performed on an example patient exhibiting a typical lesion appearance. The average across patients was not taken due to differences in lesion volume.

FIGURE 1

*Signal intensity change analysis*

The FIRST automatic segmentation tool was used to obtain pre- and post- operative thalamus segmentations on MPRAGE images.[11] MPRAGE images were registered to T2-weighted for both pre-and post-operative timepoints using FLIRT.[12,13] A lesion cost function weighting was used for post-operative image registration. These transformations were then applied to the FIRST thalamus segmentations to align them to T2-weighted images. Histogram values were extracted for n=10 bins (0-2000 intensity range) and averaged across 7 participants (those that had the required images) to produce histograms showing T2-weighted signal intensity changes in the thalamus following thalamotomy.

*Lesion volumetry*

Volumetric lesion segmentation was performed manually on all slices with the lesion using FSLeyes.[14] For early scans, FLAIR and T2-weighted lesions were segmented into 3 concentric regions previously described by Wintermark et al.[15]: I, the necrotic lesion core (hypointense); II, cytotoxic oedema (markedly hyperintense); and III, the surrounding perilesional oedema (moderately hyperintense). At the later scans, these zones were not present and so the entire visible lesion was segmented (lesions were only visible on T2-weighted, FLAIR and SWI). The volumes of each lesion mask were obtained in $mm^3$.

*Lesion localisation*

Lesion location was determined following brain extraction (using BET)[16] by a two-stage registration of (i) T2-weighted images to the corresponding pre-procedural T1-weighted image (linear registration using FLIRT with a lesion cost function weighting),[12,13] and (ii) registration of the T1-weighted MPRAGE image to the Montreal Neurological Institute (MNI) template (non-linear registration using FNIRT).[17] The transforms obtained from registration were applied to the lesion segmentations using nearest neighbour interpolation (final image resolution was 1mm isotropic). Right-sided lesions were flipped at the mid-sagittal plane to allow comparison of the anatomical location of all lesions. Lesion location was determined for each patient by calculating percentage overlap of lesion voxels with a VIM atlas (Distal atlas, Lead-DBS)[18] and FGATIR hypointensity template (template of a recently identified hypointensity on FGATIR at the base of the thalamus).[19]

Statistical analysis

Statistical analysis was performed using IBM SPSS Statistics (Version 28.0.0.0). Two repeated measures ANOVAs with pairwise comparisons (Bonferroni adjusted) were applied to the volumetric data. One ANOVA examined the effect of sequence and lesion number on early lesion zone volumes for the full cohort with T2 and FLAIR data (n=10), while the other ANOVA was applied to the cohort with 2 post-operative scans (n=5) to analyse the effect of sequence and time on total lesion volume. All data are presented as a mean ± standard deviation (SD).

## Results

**All patients had clinically meaningful tremor improvement post-operatively.**

**TABLE 1**

Participants were 12 patients (mean age of 74.6 ± 3.4 years; 4 females) who underwent unilateral RF thalamotomy at St George's Hospital, London, from 2017 to 2022. All patients had a pre-operative diagnosis of medication-refractory PD (n=10) or ET (n=2).

All 12 patients had clinically meaningful tremor improvement postoperatively, as assessed by a neurologist (CGI score of between 1 and 3). 5 patients presented with persistent adverse effects that included 4 instances of balance disturbances and a case of worsening mobility due to parkinsonism progression (Table 1). No repeat procedures were performed.

**Lesion characteristics and signal intensity varied by MRI sequence.**

**FIGURE 2**

All 12 patients had a preoperative scan and a postoperative scan between 4- and 37- days following surgery (mean of 16 days). 5 of these patients had an additional scan approximately 5 months to a year following thalamotomy (approx. 8 months postoperatively on average).

The postoperative MR images (MPRAGE, T2-weighted, FLAIR, FGATIR and SWI sequences) of 12 patients who underwent thalamotomy for tremor were analyzed. Lesions

were incompletely visualized on MPRAGE whereas T2-weighted, FLAIR and FGATIR images showed a hypointense necrotic core surrounded by a region of hyperintense oedema (see Fig. 2B for example). A small sphere of hyperintensity could also be seen at the center of the necrotic core in the majority of patients (7/10 on T2-weighted images). T2-weighted and FLAIR scans had a clear differentiation of the core versus oedema (Fig 2C: signal intensity differences of 0.35 and 0.51, respectively, in the example lesion), as well as the oedema from surrounding tissue. In contrast, FGATIR did not clearly distinguish between oedema and healthy tissue (see Fig 2B).

Presentation of the lesion center on SWI was typically isointense compared to the surrounding thalamus, with a well-defined hypointense edge. The marked hypointensity on SWI images corresponded to the area surrounding the necrotic core on other sequences (see Fig 2C at 3-4 mm radius from the center) and allowed for a clear segmentation of the lesion.

**T2-weighted images showed a clear demarcation of lesion features of necrotic core, cytotoxic oedema and perilesional oedema.**

FIGURE 3

4 out of 12 participants presented with two levels of oedema visible on T2-weighted and FLAIR images (Fig 3B); a strong hyperintense region of cytotoxic oedema and a moderately hyperintense region of perilesional oedema (see Fig 3A for example). This has been previously described[15] and was optimally demarcated on T2-weighted images. Nevertheless, the changes in signal between the pre- and post- operative scans (Fig. 3D) do not show a discrete cut off and hence lesions required manual rather than automatic segmentation.

We performed a volumetric analysis of T2-weighted lesion features by manual segmentation. Volume of the necrotic core was consistent across participants (mean of 90 ± 31 $mm^3$), while cytotoxic oedema demonstrated higher variance (mean of 433 ± 172 $mm^3$). For patients that presented with perilesional oedema (n=5), its volume tended to be greater than for cytotoxic oedema and varied more considerably between participants (mean of 2190 ± 1837 $mm^3$). Neither the presence of perilesional oedema nor its volume was associated with postoperative complications (3 out of 5 participants with perilesional oedema did not have chronic side effects). One participant who received 3 lesions presented with a significantly greater total lesion volume compared to the other participants (5408 $mm^3$ versus mean of 911 ± 535 $mm^3$) and was excluded from further group level analysis. Clinically, this larger volume was associated with 'much improved' tremor but mild balance disturbances (Table 1, Participant 07).

Comparison of T2-weighted and FLAIR lesion volumes showed that while the volumes of the lesion core were consistent across T2-weighted and FLAIR images (p = 0.394), FLAIR had a larger area of hyperintense cytotoxic oedema (T2-weighted mean = 433 ± 172 $mm^3$; FLAIR mean = 586 ± 221 $mm^3$, p = 0.005). This greater hyperintensity on FLAIR may have contributed to the difficulty in distinguishing between the two levels of oedema using this sequence.

**Early lesion cores were consistently located in the VIM and overlapped with an FGATIR hypointensity template**

FIGURE 4

Lesion necrotic cores were well-localized to the VIM nucleus of the thalamus, with cytotoxic and perilesional oedema expanding out of this area (Fig 4A). 7/9 lesion necrotic cores overlapped with the VIM atlas with on average, 45.2% of core voxels showing an overlap.

8 out of 9 lesion necrotic core segmentations overlapped to some degree with the FGATIR hypointensity template (mean overlap: 7.7 ± 6.0 % of lesion voxels).

**Multiple lesions were associated with more cytotoxic oedema compared to single lesions**

**FIGURE 5**

Patients received either a single lesion (n=5) or multiple lesions (n=7) according to intra-operative findings, with a cumulative heating time of 30-210 seconds. After exclusion of the outlier and participants with no T2-weighted image, there were 4 participants with single lesions and 5 with multiple lesions.

Size of the necrotic core and total oedema volume, which included the perilesional oedema for those that had it, did not significantly vary by lesion number ($p = 0.122$ and $p = 0.969$, respectively). Multiple lesions were associated with greater cytotoxic oedema compared to single lesions. This difference was statistically significant, though should be interpreted with caution due to the low sample size (T2-weighted mean: 537 ± 112 $mm^3$ versus 302 ± 146 $mm^3$, $p=0.028$).

**Lesion volume reduced significantly over time and appeared to stabilise at approximately 6 months post-procedure.**

**FIGURE 6**

Lesion volumes significantly reduced over time and apparently stabilized at around 6 months post-procedure, as indicated by a reduction in volume variance between patients at early and late scans (50 $mm^3$ vs 535 $mm^3$ SD, Fig 6A). For those patients who underwent multiple postoperative scans (n=5), total lesion volume reduced on average by 90% between the earlier (12 ± 3 days post-surgery) and later (254 ± 131 days post-surgery) timepoint (mean of 918 ± 517 versus 75 ± 50 $mm^3$, p=0.023). The volume and location of lesions after 5 months were comparable to those of the lesion core at earlier timepoints, indicating a resolution of oedema over time while the necrotic core remained (Fig 6A & B).

Figure 6C shows a comparison of lesion volumes from different sequence segmentations at the later timepoint. Lesions were not discernable on MPRAGE and FGATIR sequences after 5 months post-procedure. T2-weighted and FLAIR lesion volumes were similar (T2-weighted mean of 75 ± 50 $mm^3$ versus 66 ± 26 $mm^3$ for FLAIR, p = 1.000) whereas SWI segmentations were larger than those of corresponding T2-weighted images (SWI mean = 123 ± 62 $mm^3$, Bonferroni corrected p value of 0.078). However, statistically, lesion volume did not significantly differ by sequence.

**Discussion**

We investigated the imaging characteristics of RF thalamotomy with the aim to better understand how lesion features are associated with time, surgical factors, and specific MRI

sequences. Improving understanding of MRI lesion characteristics following thalamotomy will inform postoperative imaging and follow-up to improve clinical outcomes and better understand lesion physiology.

**Early scan**

The typical early (< 5 weeks post-procedure) MR lesion characteristics present in T2-weighted, FLAIR and FGATIR sequences following RF thalamotomy for tremor were a hypointense necrotic core surrounded by a hyperintense region of cytotoxic oedema. In 5 out of 12 participants, a moderately hyperintense area of perilesional oedema was also visible on T2-weighted and FLAIR sequences. These MR characteristics of three concentric lesion zones are consistent with those previously reported for both RF and magnetic resonance guided focused ultrasound (MRgFUS) thalamotomy.[15,21,22] It is notable that we also observed a small region of hyperintensity within the necrotic which is not accounted for in the volumetric analysis, and is most likely cystic in nature.

Regarding lesion location, in line with data demonstrating good spatial accuracy of stereotactic thalamotomy techniques, our findings showed good localisation of lesions to the VIM of the thalamus.[4,21,23,24] In addition, most lesion necrotic cores (8/9) showed some overlap with an atlas of a recently identified FGATIR hypointensity, thought to represent the dentatorubrothalamic tract (DRT).[19] Recent evidence suggests that disruption of the DRT is associated with tremor improvement.[25,26] Our finding further validates the potential of the FGATIR hypointensity as a visual marker for direct surgical targeting in thalamotomy for tremor.[19]

In contrast to previous reports following MRgFUS,[15,21] perilesional oedema was not observed across all of our participants. Given that perilesional oedema significantly increases the total lesion volume and is associated with post-operative complications,[21] our findings indicate that RF offers a more focused and predictable lesioning compared to MRgFUS, which would be expected to result in fewer post-operative deficits. In support of this, previously reported lesion sizes are smaller for RF[3] compared to MRgFUS.[27] The possible difference in predictability of lesions between these techniques may be related to the increased number of variables, e.g., skull density ratio, which affect the resultant lesion when using ultrasound.[28,29] Alternatively, as 10 out of 12 participants had their first scan more than 1-week following surgery when perilesional oedema has been reported to be resolved,[5,15] our participants may in fact have developed perilesional oedema which had dissipated by the time of their first scan. Therefore, a direct comparison of MRgFUS and RF thalamotomy is needed for better understanding of the surgical factors associated with development of perilesional oedema. This may help to reduce postoperative complications in the future.

Comparison of our volumetric findings with those of previous studies are difficult due to the variability in measurement technique and time of scan. However, lesion volumes appeared to be within normal ranges described by previous literature.[21–23] It has been previously shown that the number of RF lesions made correlates positively with lesion volume.[30] Our results indicate that this may be more specifically related to a greater volume of cytotoxic oedema development following multiple lesion creation. While participants with 2 compared to 1 lesion tended to have a larger cytotoxic oedema volume, we found no association between lesion number and volume of the necrotic core or perilesional oedema.

Early lesion characteristics were best demarcated on T2-weighted images, which showed a clearer distinction between cytotoxic and perilesional oedemas compared to FLAIR. The combination of T1- and T2- weighting in FLAIR imaging, as well as it's lower spatial resolution may have contributed to the observed differences in boundaries between these sequences. Despite the visible distinction of oedemas in T2-weighted images, it is notable that the lack of a discrete difference in signal between pre- and post- operative T2-weighted scans suggest that lesion segmentation currently is best appreciated with manual segmentation. While lesions were well defined on SWI images by a strong hypointense edge which allowed for a clear lesion segmentation, this sequence may be less useful in the early stages following thalamotomy when presence of oedema, not visible on SWI, is clinically relevant for explaining some transient postoperative side effects.[21]

**Late scan**

Lesions significantly reduced in volume over time and appeared to stabilise in size at approximately 6 months after surgery. This is similar to a previous approximation of 7 months for stabilisation of RF thalamotomy lesions.[22] Lesion size at the second postoperative scan was comparable to that of the necrotic core at the first scan, suggesting the reduction in volume over time was a resolution of the associated oedema. Overall, our findings suggest that scanning patients at 6 months post-procedure is reasonable for understanding the permanent effects of thalamotomy.

In contrast to previous findings for MRgFUS, reporting that lesions are often not discernible on T2-weighted images after 6 months,[29,31] we found a visible T2-weighted lesion on all 5 patients who underwent a second postoperative scan (> 5 months after surgery). However,

SWI lesion segmentations were larger than those of T2-weighted (Fig 6C), suggesting that this sequence may be more optimal for visualising lesions at later timepoints. The better visibility of lesions on SWI is likely due to its sensitivity in detecting the presence of paramagnetic compounds such as hemosiderin remnants.[32] In support of this, it has been demonstrated that SWI lesions remain discernible after MRgFUS when the same lesions are no longer visible on T2-weighted images.[31] Given the association between shrinking of lesions over time and relapse of tremor,[31,33] tracking SWI lesion volume and discernability may be useful for informing the need for repeat unilateral treatment. Indeed, this relationship may not be captured on T2-weighted images where patients have shown sustained clinical efficacy despite the absence of a T2-visible lesion.[5] However, it is notable that lesions appear larger on SWI due to blooming artifacts.[34]

**Limitations**

Our interpretation is limited by the fact that we grouped images acquired at different timepoints for analysis of early (4-37 days post-procedure) and late scans (175-449 days post-procedure). We did not seek to relate MRI lesion characteristics to clinical outcome in this study. However, we are standardising our clinical follow-up as part of a multi-centre registry study (RAPID-CNS, Boston Scientific) which would enable such analysis in future. Regarding clinical data, we are planning to use the Parkinson's Kinetigraph (PKG, Global Kinetics Corporation™) to offer a quantitative appraisal of symptom benefit while minimising inconvenience and logistics.[35] With regards to adverse events, while the reported rates are not low, this is most likely a feature of our assessments being undertaken by an independent neurologist and reported in a manner to maximise sensitivity. Furthermore, the severity of the impairments was often mild and functionally had minimal sequelae.

Additionally, the majority of these effects readily resolved, and indeed effects were almost exclusively mild balance disturbances that would be difficult to discern from the effects of underlying disease progression. Finally, inherent differences in spatial resolution between sequences will likely affect delineation of the lesion, impacting on direct comparisons between sequences.

## Conclusions

Radiofrequency thalamotomy produces focused and predictable lesion imaging characteristics, with lesion volume significantly reducing over time and apparently stabilising at approximately 6 months post-procedure. Therefore, scanning patients in the immediate post-operative period and then at 6 months is clinically relevant for understanding the transient and permanent effects of thalamotomy. T2-weighted images are useful for demarcation of early lesion features including oedema, while SWI may be more useful for visualising lesions at later timepoints when discernability reduces on other sequences. Lesioning has experienced a renaissance driven by MRgFUS and the recognition of its relative merits viz a viz DBS. These data highlight the forgotten potential of radiofrequency lesioning, provide a valuable contribution to understanding the pathophysiology of brain lesions, and a noteworthy resource with which to compare the MRI characteristics of different lesioning techniques.

## Data availability

The data that support the findings of this study are available from the corresponding author, upon reasonable request.

**Acknowledgments**

BI is funded by Life after Paralysis.

**Funding**

This work was supported by the Royal College of Surgeons of Edinburgh and St George's University of London MCS grant.

**Competing interests**

F.M.: Speaking honoraria from Abbvie, Medtronic, Bial, Merz; Travel grants from the International Parkinson's disease and Movement Disorder Society; Advisory board fees from Merz and Boston Scientific; Consultancy fees from Merz, Boston Scientific and Bial; Research support from NIHR, UKRI, Boston Scientific, Merz and Global Kynetic; Royalties from Springer for the book "Disorders of Movement"; member of the editorial board of Movement Disorders, Movement Disorders Clinical Practice, European Journal of Neurology, Journal of Neurology. E.P.: chief investigator of RAPID-CNS.

**References**

1. Schneider SA, Deuschl G. The Treatment of Tremor. *Neurotherapeutics*. 2014;11(1):128-138. doi:10.1007/s13311-013-0230-5
2. Nagaseki Y, Shibazaki T, Hirai T, et al. Long-term follow-up results of selective VIM-thalamotomy. *J Neurosurg*. 1986;65(3):296-302. doi:10.3171/jns.1986.65.3.0296
3. Hirai T, Miyazaki M, Nakajima H, Shibazaki T, Ohye C. The correlation between tremor characteristics and the predicted volume of effective lesions in stereotaxic

nucleus ventralis intermedius thalamotomy. *Brain*. 1983;106(4):1001-1018. doi:10.1093/brain/106.4.1001

4. Schreglmann SR, Krauss JK, Chang JW, Bhatia KP, Kägi G. Functional lesional neurosurgery for tremor: A systematic review and meta-analysis. *J Neurol Neurosurg Psychiatry*. 2018;89(7):717-726. doi:10.1136/jnnp-2017-316302
5. Elias WJ, Huss D, Voss T, et al. A Pilot Study of Focused Ultrasound Thalamotomy for Essential Tremor. *N Engl J Med*. 2013;369(7):640-648. doi:10.1056/nejmoa1300962
6. Tasker RR. Deep brain stimulation is preferable to thalamotomy for tremor suppression. *Surg Neurol*. 1998;49(2):145-153. doi:10.1016/S0090-3019(97)00459-X
7. Hassler R. Architectonic organization of the thalamic nuclei. In: Schaltenbrand G, Wahren W, eds. *Stereotaxy of the Human Brain*. 2nd ed. ; 1977.
8. Sudhyadhom A, Haq IU, Foote KD, Okun MS, Bova FJ. A high resolution and high contrast MRI for differentiation of subcortical structures for DBS targeting: The Fast Gray Matter Acquisition T1 Inversion Recovery (FGATIR). *Neuroimage*. 2009;47(SUPPL. 2):T44-T52. doi:10.1016/j.neuroimage.2009.04.018
9. Woolrich MW, Jbabdi S, Patenaude B, et al. Bayesian analysis of neuroimaging data in FSL. *Neuroimage*. 2009;45(1 Suppl):S173-S186. doi:10.1016/j.neuroimage.2008.10.055
10. Smith SM, Jenkinson M, Woolrich MW, et al. Advances in functional and structural MR image analysis and implementation as FSL. *Neuroimage*. 2004;23(SUPPL. 1):208-219. doi:10.1016/j.neuroimage.2004.07.051
11. Patenaude B, Smith SM, Kennedy DN, Jenkinson M. A Bayesian model of shape and appearance for subcortical brain segmentation. *Neuroimage*. 2011;56(3):907-922. doi:10.1016/j.neuroimage.2011.02.046

12. Jenkinson M, Bannister P, Brady M, Smith S. Improved Optimization for the Robust and Accurate Linear Registration and Motion Correction of Brain Images. *Neuroimage*. 2002;17(2):825-841. doi:10.1006/nimg.2002.1132

13. Jenkinson M, Smith S. A global optimisation method for robust affine registration of brain images. *Med Image Anal*. 2001;5(2):143-156. doi:10.1016/S1361-8415(01)00036-6

14. McCarthy P. FSLeyes. 2021. doi:10.5281/zenodo.6511596

15. Wintermark M, Druzgal J, Huss DS, et al. Imaging findings in mr imaging-guided focused ultrasound treatment for patients with essential tremor. *Am J Neuroradiol*. 2014;39(5):891-896. doi:10.3174/ajnr.A3808

16. Smith SM. Fast robust automated brain extraction. *Hum Brain Mapp*. 2002;17(3):143-155. doi:10.1002/hbm.10062

17. Andersson JLR, Jenkinson M, Smith S. Non-linear registration, aka spatial normalization. 2010.

18. Ewert S, Plettig P, Li N, et al. Toward defining deep brain stimulation targets in MNI space: A subcortical atlas based on multimodal MRI, histology and structural connectivity. *Neuroimage*. 2018;170(2017):271-282. doi:10.1016/j.neuroimage.2017.05.015

19. Neudorfer C, Kroneberg D, Al-Fatly B, et al. Personalizing Deep Brain Stimulation Using Advanced Imaging Sequences. *Ann Neurol*. 2022:1-16. doi:10.1002/ana.26326

20. Allen M, Poggiali D, Whitaker K, Marshall TR, Kievit RA. Raincloud plots: A multi-platform tool for robust data visualization. *Wellcome Open Res*. 2019;4:1-52. doi:10.12688/wellcomeopenres.15191.1

21. Harary M, Essayed WI, Valdes PA, McDannold N, Cosgrove GR. Volumetric analysis of magnetic resonance-guided focused ultrasound thalamotomy lesions. *Neurosurg*

*Focus*. 2018;44(2):1-8. doi:10.3171/2017.11.FOCUS17587

22. Tomlinson FH, Jack CR, Kelly PJ. Sequential magnetic resonance imaging following stereotactic radiofrequency ventralis lateralis thalamotomy. *J Neurosurg*. 1991;74:579-584.

23. Kapadia AN, Elias GJB, Boutet A, et al. Multimodal MRI for MRgFUS in essential tremor: Post-treatment radiological markers of clinical outcome. *J Neurol Neurosurg Psychiatry*. 2020;91(9):921-927. doi:10.1136/jnnp-2020-322745

24. Horisawa S, Fukui A, Nonaka T, Kawamata T, Taira T. Radiofrequency Ablation for Movement Disorders: Risk Factors for Intracerebral Hemorrhage, a Retrospective Analysis. *Oper Neurosurg*. 2021;21(3):143-149. doi:10.1093/ons/opab169

25. Chazen JL, Sarva H, Stieg PE, et al. Clinical improvement associated with targeted interruption of the cerebellothalamic tract following MR-guided focused ultrasound for essential tremor. *J Neurosurg*. 2018;129(2):315-323. doi:10.3171/2017.4.JNS162803

26. Dembek TA, Petry-Schmelzer JN, Reker P, et al. PSA and VIM DBS efficiency in essential tremor depends on distance to the dentatorubrothalamic tract. *NeuroImage Clin*. 2020;26:102235. doi:10.1016/j.nicl.2020.102235

27. Boutet A, Ranjan M, Zhong J, et al. Focused ultrasound thalamotomy location determines clinical benefits in patients with essential tremor. *Brain*. 2018;141(12):3405-3414. doi:10.1093/brain/awy278

28. Binder DK, Shah BB, Elias WJ. Focused ultrasound and other lesioning in the treatment of tremor. *J Neurol Sci*. 2022;435:120193. doi:10.1016/j.jns.2022.120193

29. Jung HH, Chang WS, Rachmilevitch I, Tlusty T, Zadicario E, Chang JW. Different magnetic resonance imaging patterns after transcranial magnetic resonance–guided focused ultrasound of the ventral intermediate nucleus of the thalamus and anterior limb of the internal capsule in patients with essential tremor or obsessive-comp. *J*

*Neurosurg*. 2015;122:162-168. doi:10.3171/2014.8.JNS132603.DISCLOSURE

30. Hirabayashi H, Hariz MI, Wrdell K, Blomstedt P. Impact of parameters of radiofrequency coagulation on volume of stereotactic lesion in pallidotomy and thalamotomy. *Stereotact Funct Neurosurg*. 2012;90(5):307-315. doi:10.1159/000338249

31. Keil VC, Borger V, Purrer V, et al. MRI follow-up after magnetic resonance-guided focused ultrasound for non-invasive thalamotomy: the neuroradiologist's perspective. *Neuroradiology*. 2020;62(9):1111-1122. doi:10.1007/s00234-020-02433-9

32. Schelhorn J, Gramsch C, Deuschl C, et al. Intracranial hemorrhage detection over time using susceptibility-weighted magnetic resonance imaging. *Acta radiol*. 2015;56(12):1501-1507. doi:10.1177/0284185114559958

33. Bruno F, Catalucci A, Arrigoni F, et al. Comprehensive evaluation of factors affecting tremor relapse after mrgfus thalamotomy: A case-control study. *Brain Sci*. 2021;11(9). doi:10.3390/brainsci11091183

34. Halefoglu AM, Yousem DM. Susceptibility weighted imaging: Clinical applications and future directions. *World J Radiol*. 2018;10(4):30-45. doi:10.4329/wjr.v10.i4.30

35. Khodakarami H, Shokouhi N, Horne M. A method for measuring time spent in bradykinesia and dyskinesia in people with Parkinson's disease using an ambulatory monitor. *J Neuroeng Rehabil*. 2021;18(1):1-17. doi:10.1186/s12984-021-00905-4

**Figure Legends:**

Figure 1 – **Example spherical regions of interest (ROIs) for one patient in the sagittal view.** ROI 1 = 0.5 mm radius sphere surrounding centre of lesion coordinate, ROI 5 = spherical area 2.5 - 3 mm from centre of lesion, ROI 11 = spherical area 5.5 – 6 mm from centre of lesion.

Figure 2 – **A, Flowchart of scanning procedure. B, Example lesion from one patient, visualized early (11 days after surgery) on MPRAGE, T2-weighted, FLAIR, SWI and FGATIR.** Images are co-registered to MPRAGE. **C, Signal intensity graph corresponding to the MR images depicted in B.** Data points show the mean signal intensity of spherical areas surrounding a seed coordinate at the centre of the lesion (see Methods). Signal intensity was normalised by dividing by the mean intensity of the surrounding intact tissue of the thalamus.

Figure 3 – **A, Example T2-weighted lesion showing volumetric segmentations of lesion zones** (necrotic core: blue; cytotoxic oedema: yellow; perilesional oedema: white) in the sagittal view. **B, Volumes of lesion zones** (necrotic core, cytotoxic oedema and perilesional oedema) on T2-weighted images at the first postoperative scan for each participant (n=10). **C, Comparison of T2-weighted and FLAIR lesion zone volumes.** An ANOVA showed that necrotic core volumes were not statistically different between T2 and FLAIR ($p = 0.394$, $F = 0.843$) whereas cytotoxic oedema differed ($p = 0.005$, $F = 18.337$). D, Histograms showing changes (pre- versus post- operative scans) to the mean signal intensity (n=7) of the thalamus on T2-weighted images as a result of the lesion.

Figure 4 - **Lesion location heatmap in MNI space** (slice locations shown in mm, color bar indicates the relationship between color and n). A, The whole lesion (blue) and necrotic core (yellow-red) segmentations from T2-weighted images (n=9) were registered to the MNI template and overlayed. The VIM of the thalamus is indicated in green (Distal medium atlas).[18] B, Overlap of T2-weighted necrotic core segmentations (red, n=9) with an FGATIR hypointensity template[19] (blue) in MNI space.

Figure 5 – **Raincloud plot[20] showing volume differences of lesion features (from T2-weighted images) between patients with 1 versus 2 lesions made.** An ANOVA with pairwise comparisons showed statistical difference values of $p = 0.122$ ($F = 3.092$) for necrotic core, $p = 0.028$ ($F = 7.579$) for cytotoxic oedema, and $p = 0.969$ ($F=0.002$) for total oedema.

Figure 6 – **A, Graph of T2-weighted lesion volume reduction over time.** Whole lesion volumes for each scan are plotted. Volumes at 'early' and 'late' timepoints are joined for patients who underwent 2 postoperative scans (n=5). An ANOVA with pairwise comparisons showed a statistical difference between 'early' and 'late' scans ($p = 0.023$, $F = 12.9$). Lesion core volumes at the early timepoint are plotted in red. **B, Change in lesion location between 1st (blue) and 2nd (red-yellow) postoperative scan for 5 patients overlayed in MNI space.** Slice location shown in mm. Color bar indicates the relationship between color and n. **C, Comparison of T2-weighted, FLAIR and SWI lesion volumes at 2nd postoperative scan** (n=5, each participant in a different colour). SWI volumes were larger than T2-weighted, but not statistically different ($p = 0.078$, $F = 14.005$, ANOVA with pairwise comparisons).

| Patient | Diagnosis | Patient CGI | Clinician CGI | Number of lesions | Early Side effects | Persistent Side effects |
|---|---|---|---|---|---|---|
| 01 | PD | 1 | 1 | 2 | None | None |
| 02 | PD | 1 | 1 | 2 | None | None |
| 03 | ET | 2 | 2 | 1 | Dysarthria and mild gait disturbances | None |
| 04 | PD | 1 | 1 | 2 | Mild worsening of previously existing balance disturbances and mild dysarthria | Mild balance disturbances |
| 05 | PD | 2 | 2 | 2 | Balance disturbances | Balance disturbances |
| 06 | PD | 1 | 1 | 2 | Delirium, dysarthria, balance disturbances | Balance disturbances |

| | | | | | | |
|---|---|---|---|---|---|---|
| 07 | PD | 2 | 2 | 3 | Mild balance disturbances, mild dysarthria and subtle left side dysmetria | Mild balance disturbances |
| 08 | PD | 1 | 1 | 1 | None | None |
| 09 | PD | 2 | 2 | 2 | Delirium | None |
| 10 | ET | 1 | 1 | 1 | Mild worsening of previously existing balance disturbances | None |
| 11 | PD | 3 | 3 | 1 | Delirium | Worsening of mobility due to parkinsonism progression |
| 12 | PD | 1 | 1 | 1 | None | None |

Table 1 - **Patient characteristics and clinical outcome measured using the clinical global impressions (CGI) scale** (1: Very much improved; 2: Much improved; 3: Minimally improved; 4: No change; 5: Minimally worse; 6: Much worse; 7: Very much worse).

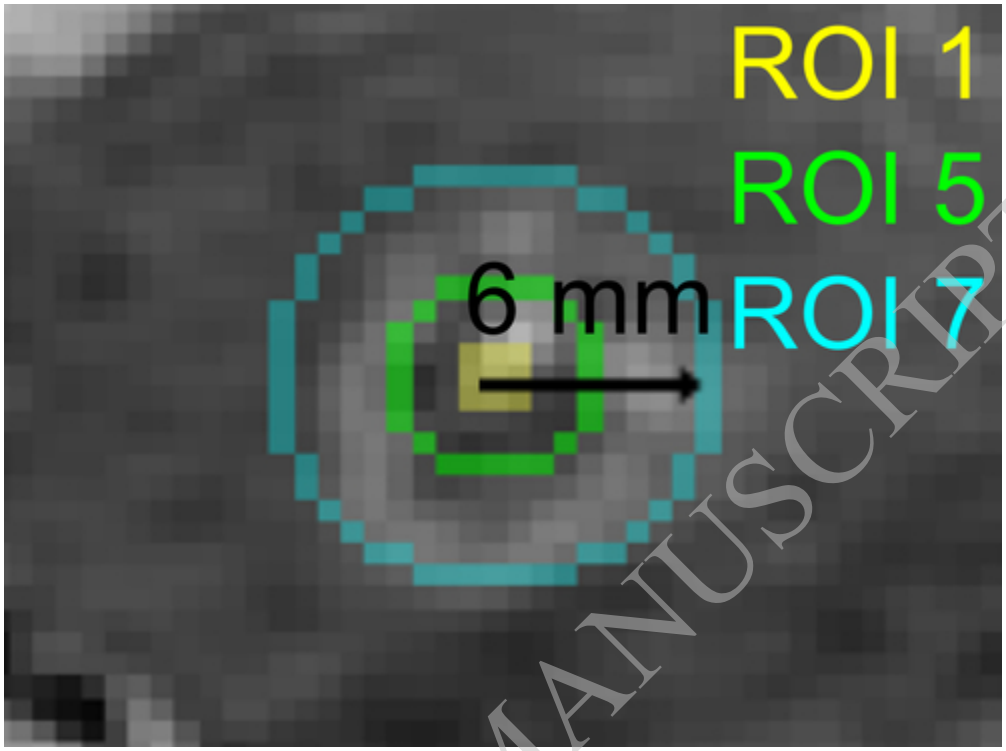


Figure 1 – Example spherical regions of interest (ROIs) for one patient in the sagittal view. ROI 1 = 0.5 mm radius sphere surrounding centre of lesion coordinate, ROI 5 = spherical area 2.5 - 3 mm from centre of lesion, ROI 11 = spherical area 5.5 – 6 mm from centre of lesion.

42x31mm (300 x 300 DPI)

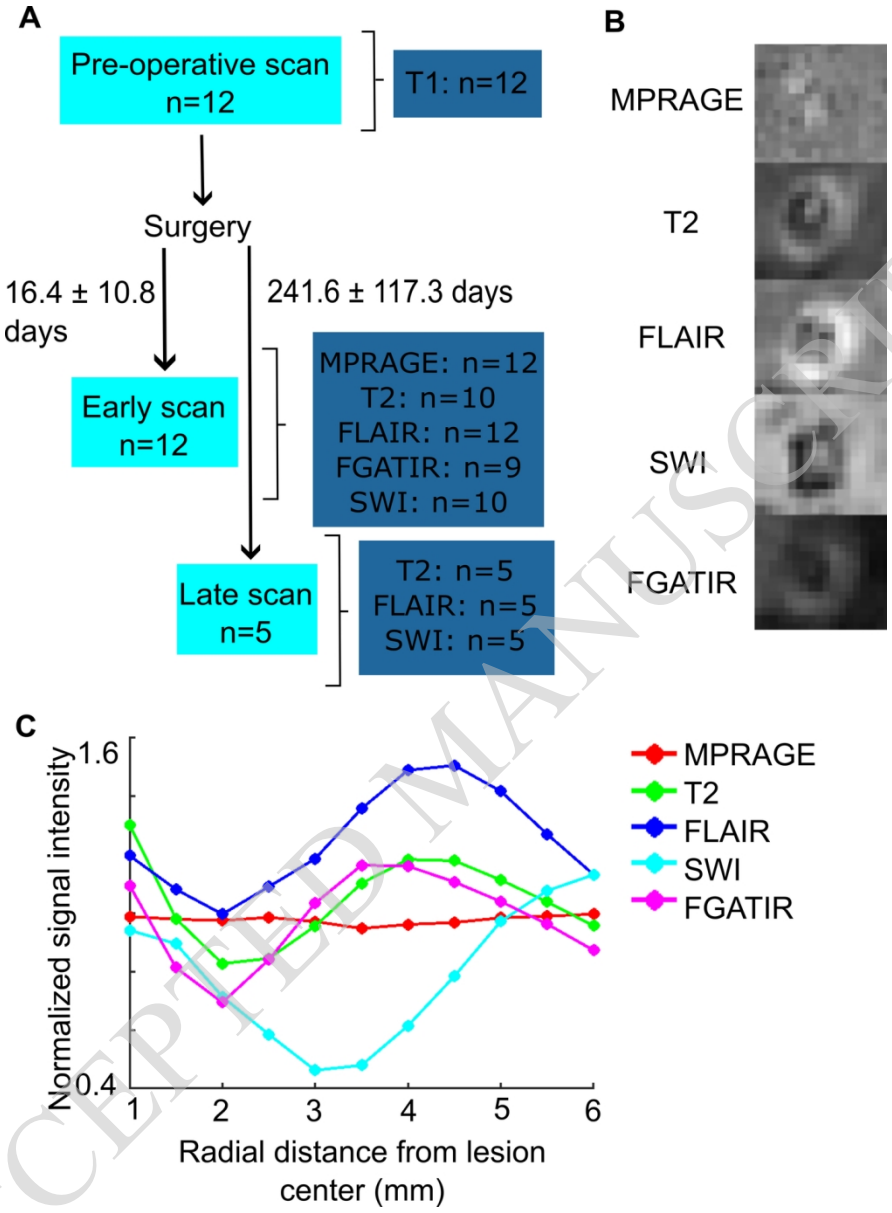


Figure 2 – A, Flowchart of scanning procedure. B, Example lesion from one patient, visualized early (11 days after surgery) on MPRAGE, T2-weighted, FLAIR, SWI and FGATIR. Images are co-registered to MPRAGE. C, Signal intensity graph corresponding to the MR images depicted in B. Data points show the mean signal intensity of spherical areas surrounding a seed coordinate at the centre of the lesion (see Methods). Signal intensity was normalised by dividing by the mean intensity of the surrounding intact tissue of the thalamus.

121x165mm (300 x 300 DPI)

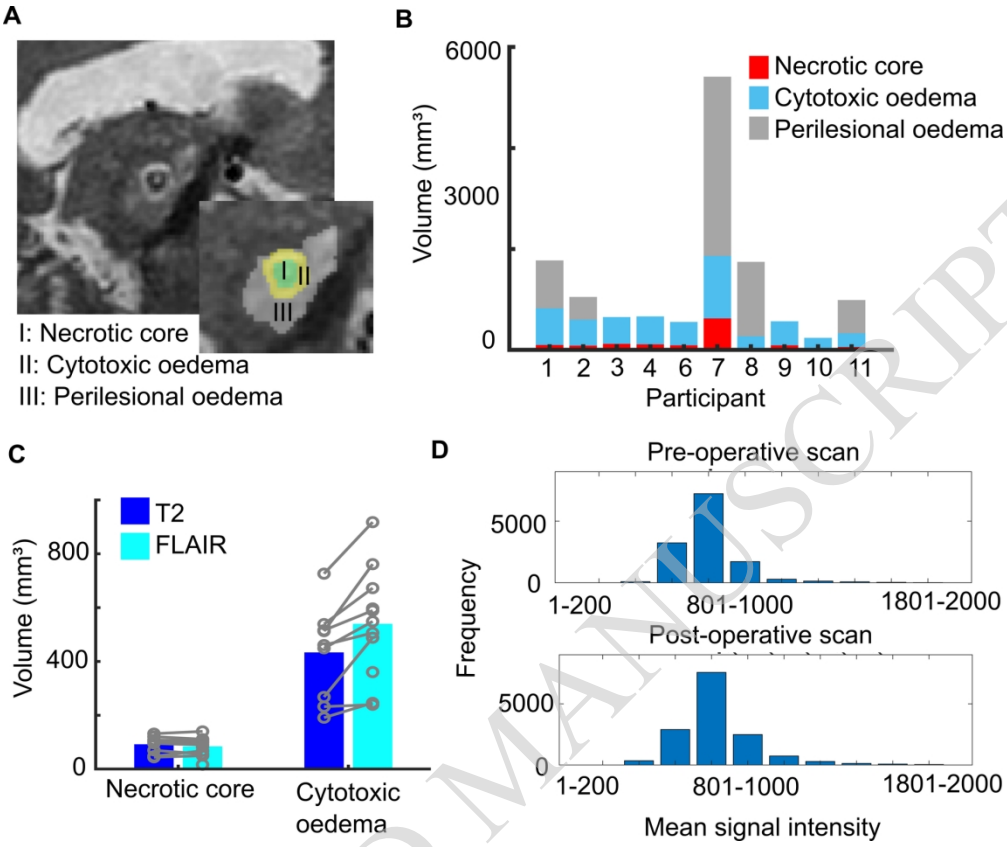


Figure 3 – A, Example T2-weighted lesion showing volumetric segmentations of lesion zones (necrotic core: blue; cytotoxic oedema: yellow; perilesional oedema: white) in the sagittal view. B, Volumes of lesion zones (necrotic core, cytotoxic oedema and perilesional oedema) on T2-weighted images at the first postoperative scan for each participant (n=10). C, Comparison of T2-weighted and FLAIR lesion zone volumes. An ANOVA showed that necrotic core volumes were not statistically different between T2 and FLAIR ($p = 0.394$, $F = 0.843$) whereas cytotoxic oedema differed ($p = 0.005$, $F = 18.337$). D, Histograms showing changes (pre- versus post- operative scans) to the mean signal intensity (n=7) of the thalamus on T2-weighted images as a result of the lesion.

166x139mm (300 x 300 DPI)

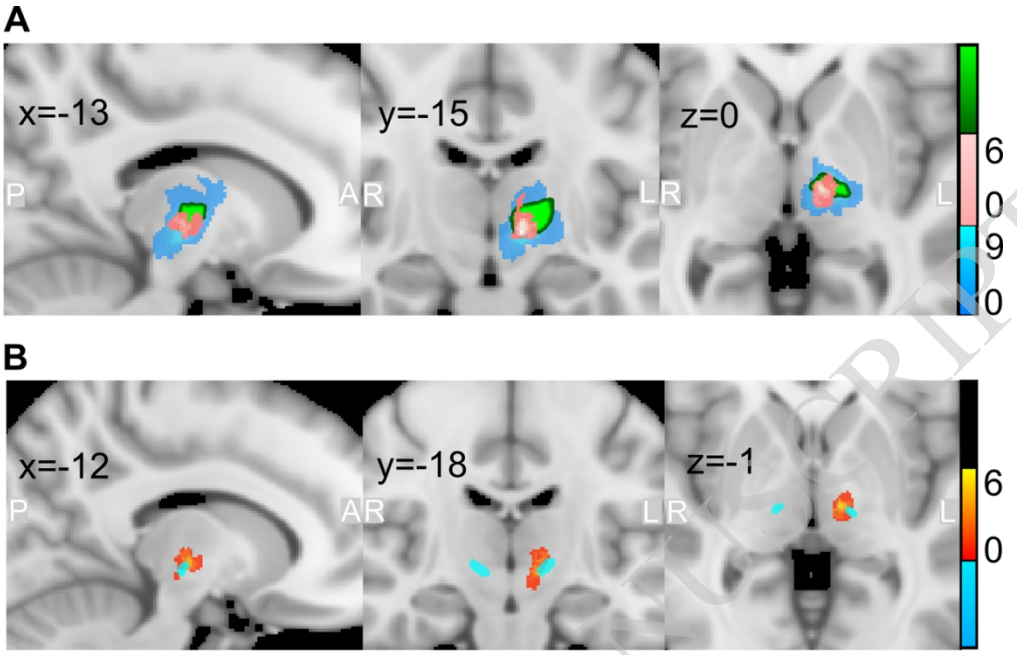


Figure 4 - Lesion location heatmap in MNI space (slice locations shown in mm, color bar indicates the relationship between color and n). A, The whole lesion (blue) and necrotic core (yellow-red) segmentations from T2-weighted images (n=9) were registered to the MNI template and overlayed. The VIM of the thalamus is indicated in green (Distal medium atlas).18 B, Overlap of T2-weighted necrotic core segmentations (red, n=9) with an FGATIR hypointensity template19 (blue) in MNI space.

117x75mm (300 x 300 DPI)

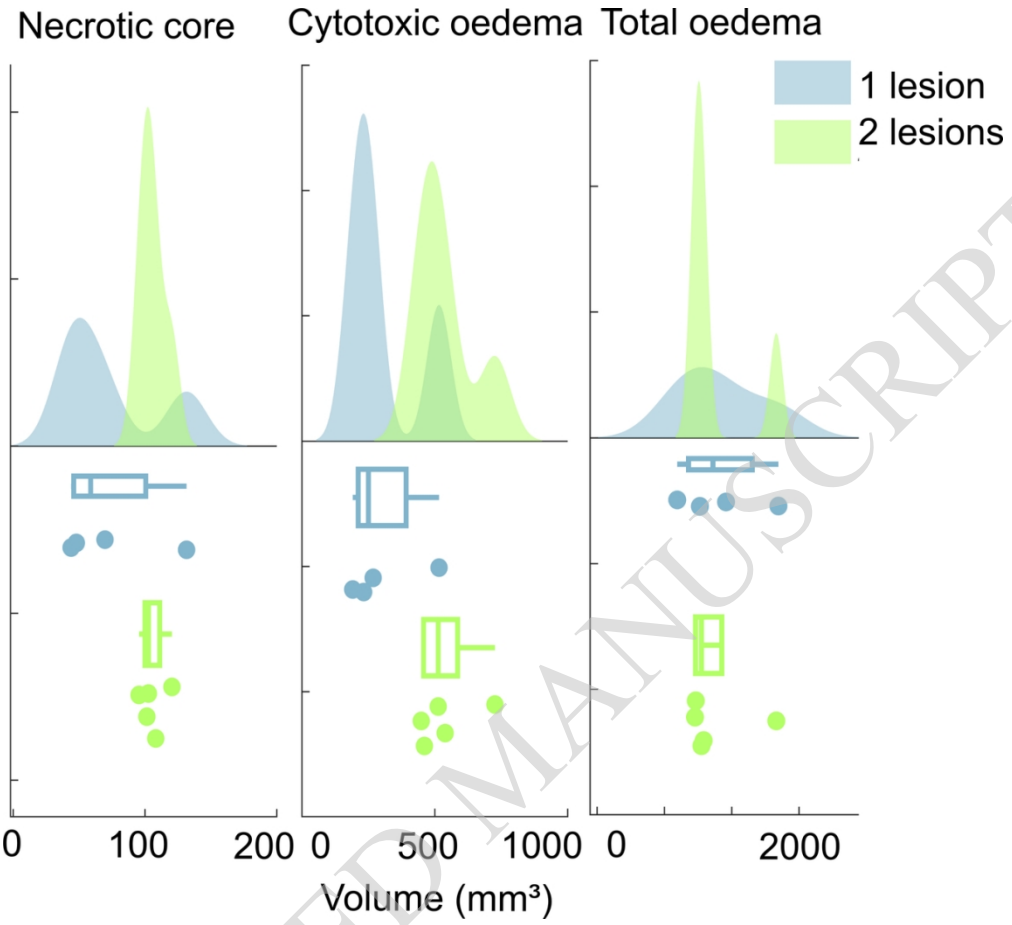


Figure 5 – Raincloud plot20 showing volume differences of lesion features (from T2-weighted images) between patients with 1 versus 2 lesions made. An ANOVA with pairwise comparisons showed statistical difference values of p = 0.122 (F = 3.092) for necrotic core, p = 0.028 (F = 7.579) for cytotoxic oedema, and p = 0.969 (F=0.002) for total oedema.

114x103mm (300 x 300 DPI)

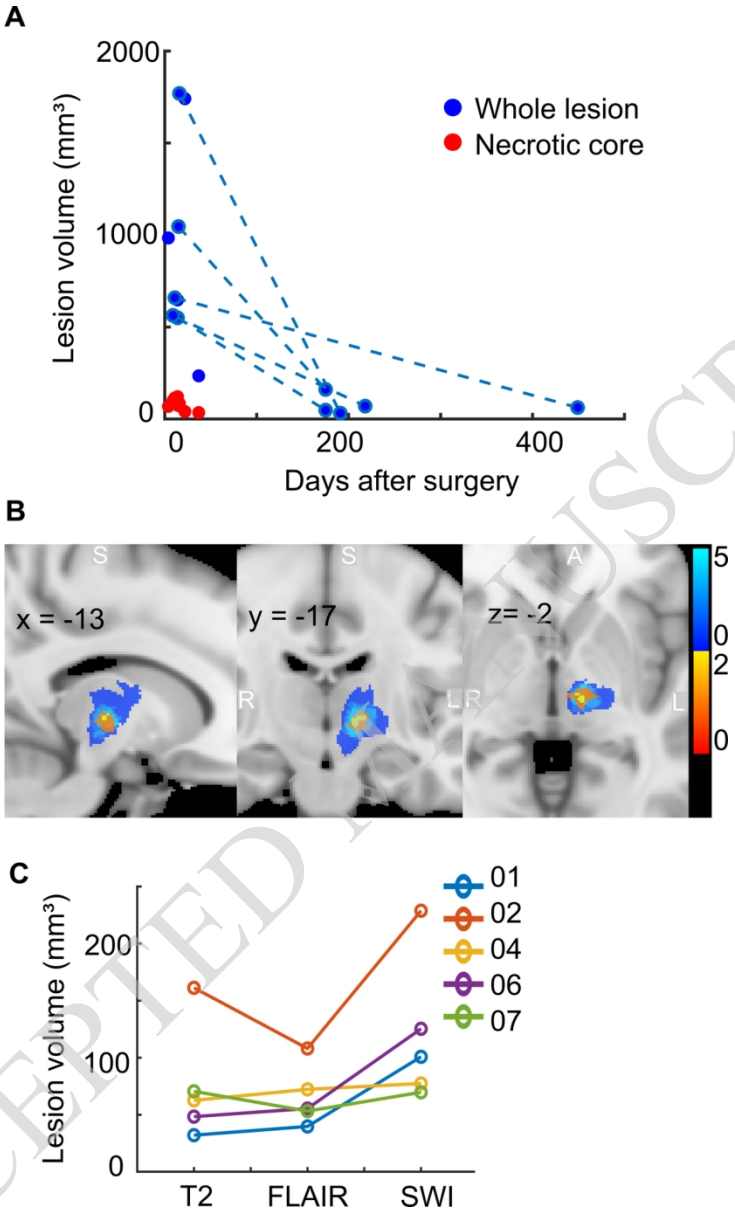


Figure 6 – A, Graph of T2-weighted lesion volume reduction over time. Whole lesion volumes for each scan are plotted. Volumes at 'early' and 'late' timepoints are joined for patients who underwent 2 postoperative scans (n=5). An ANOVA with pairwise comparisons showed a statistical difference between 'early' and 'late' scans (p = 0.023, F = 12.9). Lesion core volumes at the early timepoint are plotted in red. B, Change in lesion location between 1st (blue) and 2nd (red-yellow) postoperative scan for 5 patients overlayed in MNI space. Slice location shown in mm. Color bar indicates the relationship between color and n. C, Comparison of T2-weighted, FLAIR and SWI lesion volumes at 2nd postoperative scan (n=5, each participant in a different colour). SWI volumes were larger than T2-weighted, but not statistically different (p = 0.078, F = 14.005, ANOVA with pairwise comparisons).

106x176mm (300 x 300 DPI)